

NASA Technical Memorandum 89858  
AIAA-87-0992

# Experimental Study of Low Reynolds Number Nozzles

(NASA-TM-89858) EXPERIMENTAL STUDY OF LOW  
REYNOLDS NUMBER NOZZLES (NASA) 13 P  
CSCL 21H

N87-20383

G3/20      Unclass  
45424

Stanley P. Grisnik and Tamara A. Smith  
*Lewis Research Center*  
*Cleveland, Ohio*

and

Larry E. Saltz  
*Rocket Research Company*  
*Redmond, Washington*

Prepared for the  
19th International Electric Propulsion Conference  
cosponsored by the AIAA, DGLR, and JSASS  
Colorado Springs, Colorado, May 11-13, 1987

The NASA logo, consisting of the word "NASA" in a bold, sans-serif font.

## EXPERIMENTAL STUDY OF LOW REYNOLDS NUMBER NOZZLES

Stanley P. Grisnik and Tamara A. Smith  
National Aeronautics and Space Administration  
Lewis Research Center  
Cleveland, Ohio 44135

and

Larry E. Saltz  
Rocket Research Company  
Redmond, Washington 98052-1012

### Abstract

High-performance electrothermal thrusters operate in a low nozzle-throat Reynolds number regime. Under these conditions, the flow boundary layer occupies a large volume inside the nozzle, contributing to large viscous losses. Four nozzles (a conical, bell, trumpet, and modified trumpet) and a sharp-edged orifice were evaluated over a Reynolds number range of 500 to 9000 with unheated nitrogen and hydrogen. The nozzles showed significant decreases in specific impulse efficiency with decreasing Reynolds number. At Reynolds numbers less than 1000, all four nozzles were probably filled with a large boundary layer. The discharge coefficient decreased with Reynolds number in the same manner as the specific impulse efficiency. The bell and modified trumpet nozzles had discharge coefficients 4 to 8 percent higher than those of the cone or trumpet nozzles. The Two-Dimensional Kinetics (TDK) nozzle analysis computer program was used to predict nozzle performance. The results were then compared to the experimental results in order to determine the accuracy of the program within this flow regime.

### Introduction

Low Reynolds number nozzles have large flow boundary layers and associated viscous losses that decrease the performance of low-thrust electrothermal propulsion devices. Thrust losses approach 30 percent in the Reynolds number range that is characteristic of high-performance resistojets and arcjets.<sup>1</sup> The one-dimensional isentropic expansion analysis used for evaluating nozzle performance losses generally agrees with experimental data within a few percent for high Reynolds number nozzles ( $\geq 10,000$ ). Because of the effects of large boundary layers at low Reynolds numbers, the isentropic expansion analysis is no longer accurate.

Earlier work in the area focused primarily on conical nozzles of varying half-angles and area ratios. It was shown that the boundary layer and associated viscous losses cause a decrease in thrust coefficient with decreasing Reynolds number. Three loss mechanisms were identified, a boundary-layer effect, a heat-transfer effect, and flow-divergence losses. The viscous losses are usually much larger than divergence losses. Low Reynolds number nozzle flow has an inviscid core displaced from the wall by a viscous boundary layer. Flow velocity in both regions is expected to be less than ideal.<sup>2</sup> Viscous and divergence losses at throat Reynolds numbers less than 1000 can reduce the overall thrust power efficiency to less than 75 percent.<sup>1</sup> When heated nozzle flow is eval-

uated, radiation and conduction losses can account for 10 to 20 percent of the input gas power.<sup>3</sup> In vacuum chambers, where the ambient pressure is sufficiently high, heat-transfer losses due to convection can also occur.<sup>4,5</sup> Under the conditions of large boundary layers and viscous losses, theoretical analysis of nozzle performance using the assumption of one-dimensional isentropic expansion is no longer accurate and must be modified.<sup>1,2,6</sup>

NASA has initiated in-house and contracted efforts to develop a high-performance, storable propellant resistojet. The potential for performance gain by minimizing nozzle losses has been identified as an area for further investigation. The purpose of the work presented in this paper was to extend the data base to include nozzles with varying outlet geometries and to examine only boundary-layer effects by using unheated gas. Four nozzles of varying divergent section geometries - conical, bell, trumpet, and modified trumpet - and a sharp-edged orifice were tested with nitrogen and hydrogen over the Reynolds number range of 500 to 9000.

Present analytical methods used for nozzle analysis have not been validated at low Reynolds numbers. The Two-Dimensional Kinetics (TDK) nozzle analysis program was run, and its results were compared to the experimental data. The TDK program evaluates two-dimensional and viscous effects on the performance of liquid propellant exhaust nozzles.<sup>7</sup> It should be noted that TDK was written for high Reynolds number flow and has not been validated in the low Reynolds number regime. The version of TDK used for this paper was version 2.4, December 1984.

The TDK program calculates gas composition in the nozzle chamber and throat, assuming chemical equilibrium. By using this information, the pressure profile within the chamber and throat are calculated from isentropic flow relations. Then, the one-dimensional nonequilibrium flow relations are integrated for the flow beginning at the converging section of the nozzle and ending at an axial station located beyond the throat plane. During this calculation, the program is instructed to assume frozen chemical composition. The results obtained in the throat section are then used to estimate two-dimensional effects in the transonic region of the nozzle throat. The purpose of these calculations is to approximate an initial data line across the nozzle throat in order to start the method-of-characteristics calculations. The method of characteristics is used to determine the properties of the flow within the divergent nozzle

and thereby calculate the loss in nozzle performance caused by flow divergence. The flow conditions along the nozzle wall, which are calculated in the method of characteristics, are used to perform a boundary-layer analysis. From this analysis, the decrement in performance due to viscous effects is obtained and subtracted from the inviscid performance to obtain the final results.

The benefit of using TDK over simple one-dimensional isentropic flow relations is that it considers gas species, divergence losses, and viscous losses. Viscous losses are determined by calculating a boundary-layer displacement thickness, assuming viscous effects at the wall, and subtracting this performance loss from the inviscid core performance calculation.

This paper presents specific impulse efficiencies and discharge coefficients of the four nozzles evaluated over a wide range of throat Reynolds numbers. Experimental measurements and analytical results are compared.

### Apparatus

#### Nozzles

Four converging-diverging nozzles with different diverging contours were tested along with a sharp-edged orifice. Nozzle 1 was a 20° half-angle cone with an area ratio of 120:1 and a throat diameter of 0.653 mm. Nozzle 2, a bell-shaped nozzle with a throat diameter of 0.711 mm, and nozzle 3, a trumpet with a throat diameter of 0.671 mm, had area ratios of 150:1 and 125:1, respectively. Nozzle 4 was a modified trumpet shape - the diverging section near the throat was a 15° half-angle cone that expanded into a trumpet with a 135:1 area ratio and a throat diameter of 0.640 mm (Fig. 1 and Table 1). The orifice was a flat plate with a sharp-edged 0.724-mm-diameter hole.

Nozzle interchangeability was simplified by using a quick-connect flange assembly with a rubber o-ring (Fig. 2(a)). The nozzles were supplied by Rocket Research Corporation in conjunction with an ongoing high-performance resistojet contract.

#### Thrust Measurement

Thrust measurements were obtained using a thrust stand capable of measuring thrust levels as low as 2.9 mN. The thrust stand consisted of a horizontal mounting plate supported by a double set of four flexure plates that allowed motion in the horizontal direction (Fig. 2(a) and (b)). The flexures were designed so that a small force produced a large displacement. This helped reduce two major thrust-measurement problems - thermal drift and vibration. The thermal expansion of the thrust stand components was small compared to the movement of the thrust stand for low-thrust tests, and the flexures had a low resonant frequency, preventing any high-frequency vibrations from reaching the thruster mounting plate. The low-frequency vibrations were removed by use of a magnetic damper assembly. The damper consisted of a permanent magnet physically attached to the thruster mounting plate and inserted into an annular electromagnet. The output of the electromagnet was dependent on the movement of the thruster mounting plate. Thrust plate movement was detected by monitoring the output of the linear variable displacement transducer (LVDT).

When movement was detected, the LVDT output was amplified and used to energize the electromagnet. A magnetic field was produced which applied a force on the permanent magnet opposing the thrust plate motion.

Various thrust ranges were measured by varying the stiffness of the flexures and, if required, the stiffness of the propellant feed tube. The feed tube, a 3.2-mm-diameter thin-walled stainless steel tube, was brought onto the thrust stand perpendicular to its axis of movement, thus acting as an additional flexure.

Calibration was performed by adding known weights to a pulley assembly that deflected the thrust stand a given amount. Thrust stand tares were small and reproducible, and the estimated thrust measurement error was less than 5 percent at low thrust (<66 mN) and less than 2 percent at higher thrust levels.

Windage effects, the influence of circulating gases in the test chamber on thrust measurement, were reduced to less than 0.1 mN by installation of a windshield between the nozzle and the thrust stand body. These effects were measured by flowing gas through an orifice that was mounted close to, but not attached to, the horizontal thruster mounting plate, and checking for any thrust plate deflection.

#### Vacuum Chamber

The vacuum chamber used had a diameter of 1.0 m and a length of 2.0 m. A 30-cm pipe connected the chamber to a  $1 \times 10^5$  liter/min lobe rotary blower that was backed by a  $2 \times 10^4$  liter/min rough pump. Typical vacuum chamber pressures varied from  $1.06 \times 10^{-1}$  to  $66.5 \text{ N/m}^2$  ( $8 \times 10^{-4}$  to 0.5 torr) depending on the thrust level selected. Tests with low Reynolds numbers (<2000) had vacuum chamber pressures of less than  $1.33 \text{ N/m}^2$  ( $10^{-2}$  torr). Pressure ratios, nozzle plenum pressure divided by vacuum chamber pressure, were kept above  $10^3$  to prevent the possibility of shock formation in the nozzle.<sup>8</sup> All measured thrust values were corrected for background pressure which amounted to less than 1 percent of the measured thrust.

#### Instrumentation

Gas flow was measured by using laminar-flow, heated-tube flowmeters that are thermally sensitive to flow rate. For a constant tube reference temperature, the gas flow rate is proportional to the current input to the tube. The low range, 0 to 5 standard liter/min, flowmeter was calibrated using a soap-bubble calibrator.<sup>9</sup> The high-range, 0 to 50 standard liter/min, flowmeter was calibrated by filling a known volume to a certain pressure over a measured time increment. Errors for the low-flow-rate meter were less than 1 percent, and, for the high-flow-rate meter, less than 3 percent.

Pressures were measured by a stainless steel diaphragm transducer. The pressure tap was located approximately 12-mm upstream of the nozzle throat. The calibration was checked before every test, and errors in measurement were less than 1 percent. Vacuum-chamber pressures were measured with a cold cathode-ion gauge; estimated measurement errors were  $\pm 20$  percent for low pressure ( $< 0.133 \text{ N/m}^2$  ( $10^{-3}$  torr)). Temperatures were measured by a

stagnation probe with a chromel-alumel thermocouple mounted in the gas stream approximately 12-mm upstream of the nozzle throat; estimated measurement errors were less than  $\pm 3$  °C.

### Procedure

The test matrix consisted of three variables - throat Reynolds number, nozzle contour, and propellant. The Reynolds number is based on throat conditions and is equal to 4 times the mass-flow rate divided by the product of  $\pi$ , viscosity, and throat diameter. There were four nozzles - a conical, bell, trumpet, and modified trumpet - and a sharp-edged orifice. The propellants used were unheated nitrogen and hydrogen. Since the tests were run at constant conditions, the Reynolds number was varied by changing the mass-flow rate. The Reynolds number range tested, 500 to 9000, spanned two thrust ranges, 2.8 to 12.0 mN and 12.0 to 60 mN.

The thrust stand was set up for one thrust range, and a propellant was selected. The nozzle was attached to the thrust stand assembly, its exit was plugged, and the fittings were checked for leaks. After ensuring that the system was leak tight, the vacuum chamber was evacuated. A mass-flow rate was set with a thrust zero taken before and after each thrust measurement. Thrust measurements were recorded twice per Reynolds number set point (flow rate). Each nozzle was run three times in random order to accurately define the thrust measurement deviations, and a thrust stand calibration check was performed before and after each nozzle change.

This procedure was followed for both propellants, over both thrust ranges, and for all nozzles. The quantities recorded were thrust, inlet gas pressure, inlet gas temperature, test cell pressure, and mass-flow rate. Thrust was corrected for test cell pressure using

$$F_c = F_m + P_a A_e \quad (1)$$

where  $F_c$  is the corrected thrust,  $F_m$  is the measured thrust,  $P_a$  is the ambient test cell pressure, and  $A_e$  is the nozzle exit area. Thrust corrections were less than 1 percent over the entire range.

The specific impulse and thrust coefficient were determined using  $F_c$ . Specific impulse efficiency  $N_{ISP}$  is the ratio of actual specific impulse (calculated from measured thrust and mass-flow measurements) to theoretical maximum specific impulse. Theoretical maximum values of specific impulse at room temperature for hydrogen and nitrogen are 300 and 78 sec, respectively. The specific impulse efficiency measures the extent of the velocity losses due to nozzle viscous and divergent effects. The discharge coefficient  $C_D$  is the ratio of measured mass-flow rate to theoretical maximum mass-flow rate. For sonic conditions at the nozzle throat,  $C_D$  is dependent on the throat boundary-layer thickness. The discharge coefficient is therefore a measure of the loss of mass-flow due to viscous effects from the nozzle throat region. For a hydrogen or nitrogen propellant at room temperature, the thrust coefficient can be expressed as

$$C_F = 1.7 C_D N_{ISP} \quad (2)$$

for nozzle area ratios between 100 and 200.<sup>6</sup> Furthermore, for an orifice plate, Eq. (2) also applies. Variations in the thrust coefficient can be readily obtained from figures displaying  $N_{ISP}$  and  $C_D$  as a function of Reynolds number (Figs. 3 to 6).

The assumptions used for the TDK analysis are

- (1) There is frozen chemical composition.
- (2) There is no loss of mass from the system.
- (3) Each component of the gas is a perfect gas.
- (4) The flow is axisymmetric (in the nozzle throat region the flow is dependent on the local wall geometry only).
- (5) There are wall viscous effects.
- (6) Core flow calculations are performed assuming inviscid, compressible gas.<sup>7</sup>

### Discussion of Results

The major loss mechanism in low Reynolds number nozzles is viscous flow loss associated with the flow boundary layer, which occupies a large volume inside the nozzle. Data exploring these losses are limited, particularly in cases of nozzles with different divergent contours. Most of the past work was performed with heated gas, which can introduce an additional heat-transfer loss mechanism. The heated-gas tests represent a more accurate comparison with actual low-thrust, high-performance resistojets and arcjets, but to understand the loss mechanisms involved each effect must be separated.

The parameters of interest for unheated flow tests are the thrust coefficient  $C_F$ , the discharge coefficient  $C_D$ , and the specific impulse efficiency  $N_{ISP}$ . Figures 3 and 4 display the analytical and experimental values of specific impulse efficiency for an orifice plate as well as for convergent-divergent nozzles. The specific impulse efficiency decreases with decreasing Reynolds number for all four nozzle contours and the orifice. In the Reynolds number range of 500 to 9000,  $N_{ISP}$  for nitrogen ranged from 80 to 90 percent, whereas for hydrogen it ranged from 70 to 90 percent. All of the nozzles gave the same performance within experimental error. It should be kept in mind that the variation of nozzle area ratios (120:1 to 150:1) affects nozzle efficiency. However, it has been shown previously that the variation in specific impulse efficiency with area ratio amounted to only 4 percent for area ratios between 100:1 and 200:1 at low (500) Reynolds numbers. As the area ratio increased, the efficiency decreased.<sup>1</sup> At higher Reynolds numbers (4000), the variation in  $N_{ISP}$  for the nozzles was only 2 percent. Although the nozzles performed the same within experimental error (5 percent), it should be pointed out that a 5-percent increase in  $N_{ISP}$  would give a 10-percent increase in thrust power. Thus, a lower input electric power would be required for a given target specific impulse, or an increased thrust level could be used.

The difference in  $N_{ISP}$  for the two gases is more pronounced than the difference in  $N_{ISP}$  for the various nozzle contours. Below Reynolds numbers of 4000, nitrogen shows a higher  $N_{ISP}$  than hydrogen, whereas at high Reynolds numbers  $N_{ISP}$  is approximately 0.88 for both gases. The maximum difference at a Reynolds number of 500 is between 5 and 12 percentage points depending on nozzle

configuration. At a Reynolds number of 500, the greatest disparity between the specific impulse efficiency of hydrogen and nitrogen was observed with the trumpet nozzle.

Murch's data<sup>1</sup> for heated nitrogen and hydrogen exhibited an  $N_{ISP}$  difference of 6 percent, which is about the same observed in Figs. 3 and 4 with a conical nozzle. The viscous flow model of Edwards and Jansson<sup>2</sup> indicates very little difference in  $N_{ISP}$  for hydrogen and ammonia for Reynolds numbers between 200 and 10 000, indicating a need for more sophisticated flow models. Comparing the different specific impulse efficiencies for the orifice shows that, within experimental error, the performance of nitrogen and hydrogen is the same. At a Reynolds number of 500,  $N_{ISP}$  for nitrogen is 54 percent and for hydrogen, 57 percent. At Reynolds numbers approaching 8000, the specific impulse efficiency for nitrogen is 66 percent and for hydrogen, 68 percent. Significant variation in  $N_{ISP}$  between nitrogen and hydrogen only occurs when the gases are expanded out of the nozzle. Evidently the hydrogen nozzles at low Reynolds numbers have a thicker boundary layer than nitrogen nozzles, or (possibly) there is condensation of the nitrogen as it expands out of the nozzle.

Hydrogen does have a negative Joule-Thompson coefficient (heats upon expansion) in this temperature-pressure range as compared to nitrogen, but the effect is too small to account for any  $N_{ISP}$  variations. It is possible that a Reynolds number based on the physical throat diameter is not the appropriate correlation parameter.

Figures 5 and 6 compare discharge coefficients  $C_D$  for both gases and all four nozzles. As can be seen, the bell and modified trumpet nozzles have higher discharge coefficients than the conical and trumpet nozzles (throat measurements are accurate to within 3 percent). The difference is approximately 4 percent at a Reynolds number of 8000 and 8 percent at a Reynolds number of 500. Since the discharge coefficient is a measure of the mass-flow rate decrease due to throat boundary-layer viscous effects, it appears as though the boundary layer is thinner for the bell and modified trumpet nozzles. For a given nozzle, the discharge coefficients produced by hydrogen and nitrogen vary by no more than 2 or 3 percent.

Back has found that the discharge coefficient depends essentially on the ratio of nozzle-throat radius of curvature to nozzle-throat radius  $r_c/r_{th}$  and is independent of inlet configuration (convergent contour). As the ratio  $r_c/r_{th}$  decreases,  $C_D$  decreases.<sup>10,11</sup> Although these results are for higher Reynolds number ranges, the same trends are seen at the lower Reynolds numbers, with the bell and modified trumpet nozzles having the highest ratio of  $r_c/r_{th}$  and, correspondingly, the highest discharge coefficients. Massier<sup>12</sup> has found no effect of plenum length (growth of boundary layer in plenum) on the discharge coefficient. Rothe<sup>13</sup> has found that, for pressure ratios (gas pressure at nozzle inlet to test cell pressure) greater than approximately 350 for a Reynolds number of 500, the test cell pressure influencing the internal flow through the thick subsonic boundary layer has no effect on the discharge coefficient. All tests were run with this pressure ratio greater than 10<sup>4</sup>.

All four nozzles had the same inlet radius of curvature (1 mm), but their outlet radii varied from 0.3 to 12 mm, with the bell nozzle having the smallest value. The nozzles had throat length-to-diameter ratios between 0.4 and 1.1, with the modified trumpet having the smallest value and thus more closely approximating a sharp-edged orifice inlet. The orifice, which had a discharge coefficient equal to or greater than the best nozzle, had no inlet or outlet radius of curvature (straight-through orifice) and had a throat length-to-diameter ratio of 0.6. It is interesting to note that the orifice was designed with no convergent section and its discharge coefficient is approximately the same as, or better than, the nozzles. An upstream convergent section is not required to provide a high discharge coefficient for a choked orifice. Rae<sup>14</sup> predicted this fact analytically by using the slender channel equations with slip boundary conditions at the wall. It appears that Back's findings of the discharge coefficient depending on  $r_c/r_{th}$  do extend into the low Reynolds number range.<sup>10,11</sup> It can be assumed that the throat boundary layer is affected by  $r_c/r_{th}$ , where a smaller inlet radius (for a given throat radius) causes the formation of a larger throat boundary layer. As the throat boundary layer increases, the ratio of mass flow through the inviscid core to the mass flow through the boundary layer decreases causing a decrease in the average throat exit-gas velocity.

Table 2 summarizes the basic parameters  $C_D$ ,  $N_{ISP}$ , and  $C_F$  for all nozzles and the orifice plate at a throat Reynolds number of 1000. Nozzle discharge coefficients are clearly independent of the gases tested. At a Reynolds number of 1000, the highest nozzle thrust coefficient obtained was 1.33 and the lowest was 1.14. Almost all thrust coefficients measured at this Reynolds number were less than the thrust coefficient calculated for isentropic flow through a choked orifice ( $C_F = 1.27$ ). This apparently indicates that all nozzles were filled with a large boundary layer. The values of  $C_F$  for the orifice plate at a Reynolds number of 1000, 0.94 to 0.97, indicate a significant departure from inviscid flow. With nitrogen propellant, the variation in the nozzle thrust coefficient for the four different nozzle configurations was within the experimental uncertainty ( $\pm 2.5$  percent).

The results of the Two-Dimensional Kinetics (TDK) nozzle analysis can be seen in Figs. 3 and 4. Numerous problems were encountered during attempts to analyze low Reynolds number nozzles with a program that was written for high-thrust, high Reynolds number nozzles. The most serious problem appeared to be that the analysis would not always converge to a Mach number of unity at the throat. When running properly, the discharge coefficients calculated were 0.95 or greater, whereas the experimental data showed that the actual  $C_D$  varied from 0.83 to 1.0. The calculated discharge coefficient departed from experimental results at Reynolds numbers below approximately 4000. It can be assumed that, at this point, the TDK method of subtracting boundary-layer effects from the inviscid core is no longer valid.

For the conical nozzle, the specific impulse efficiency was predicted fairly well to a Reynolds number of 3000, after which substantial departure

from the experimental data resulted. It should be noted that this is the approximate location where the calculated discharge coefficient began to deviate from the experimental results. Results for the bell-shaped nozzle were inaccurate at every point. For the single point that was able to be run for the modified trumpet nozzle, the results were as accurate as in the conical case. No analysis was possible for the trumpet nozzle as the throat Mach number would not converge to unity.

The program did predict large displacement thicknesses at the nozzle exit (Fig. 7). The displacement thickness is the distance by which the solid surface would have to be displaced to maintain the same mass-flow rate as that of a frictionless flow. At a Reynolds number of 4000, the displacement thickness was about 40 percent of the exit plane area for the conical nozzle, 37 percent for the bell, and 67 percent for the modified trumpet. The values of thrust coefficient obtained for the conical, bell, and modified trumpet nozzles at a Reynolds number of 4000 were 1.41, 1.48, and 1.48, respectively. The calculated values of  $C_F$  are all large enough to indicate the existence of an inviscid core, but the experimental data are not consistent with the TDK results. The TDK code needs refinements in calculating the sonic conditions at the throat for the low Reynolds numbers. The method of subtracting the boundary-layer viscous effects from the inviscid core performance must also be refined.

#### Concluding Remarks

Four nozzles (a conical, bell, trumpet, and modified trumpet) and a sharp-edged orifice were evaluated over a Reynolds number range of 500 to 9000 with unheated nitrogen and hydrogen. The boundary-layer viscous losses were examined in both the divergent section and throat section of the nozzles. The nozzles showed significant decreases in specific impulse efficiency with decreasing Reynolds number. We conclude that changes in the divergent contour do not effect the viscous and divergent losses to any appreciable extent. At Reynolds numbers less than 1000, all four nozzles were probably filled with a large boundary layer.

There appears to be an effect of gas species on the viscous and divergent losses with Reynolds number. At a Reynolds number of 500, nitrogen performs approximately 5 to 12 percent better than hydrogen, depending on nozzle configuration. At the higher Reynolds numbers (>4000), the difference is within 3 percent. The difference in specific impulse efficiency does not appear when testing the orifice. This difference is related to the expansion process taking place in the divergent portion of the nozzles.

The discharge coefficient decreases with Reynolds number in the same manner as the specific impulse efficiency, but the gas species has very little effect on the discharge coefficient. The bell and modified trumpet nozzles, with higher ratios of inlet radius of curvature to throat radius, have 4 to 8 percent higher discharge coefficients than the cone or trumpet nozzles.

A comparison of the experimental results to the Two-Dimensional Kinetics (TDK) nozzle analysis predicted results indicates that better predictions

for the discharge coefficient are needed along with refinements in calculating the sonic conditions in the nozzle throat for Reynolds numbers below approximately 4000. The incorporation of viscous effects by subtracting the boundary-layer viscous losses from the inviscid core performance calculations is insufficient to account for the large viscous losses at the low Reynolds numbers. A more adequate method of accounting for viscous losses is needed.

Although the divergent section geometry has little effect on the specific impulse efficiency, a 5-percent increase would provide a 10-percent increase in thrust power per thruster. This would amount to a substantial payback for a satellite system composed of numerous thrusters.

The knee of the specific impulse efficiency curve falls in the region that is representative of the Reynolds number regime in which high-performance electrothermal thrusters operate. This region is important for two reasons. Satellite systems operate in a blowdown mode where the propellant flow rate decreases with use. Consequently, as the satellite ages its performance will decrease (following the specific impulse efficiency curve). There is also a trade off (for a given flow rate) between specific impulse efficiency and thruster chamber high-temperature creep. Large nozzles (large throat diameters) decrease the thruster operating pressure, thus decreasing the creep problems of high-temperature materials. However, there is a corresponding decrease in Reynolds number and, therefore, a decrease in specific impulse efficiency.

More analytical work needs to be done in this Reynolds number regime to aid in evaluating the above tradeoffs from a systems standpoint.

#### Acknowledgment

The authors gratefully acknowledge the work done by Thomas W. Haag of NASA Lewis Research Center in developing the thrust stand used in this investigation.

#### References

1. Murch, C.K., Broadwell, J.E., Silver, A.M., and Marcisz, T.J., "Low-Thrust Nozzle Performance," AIAA Paper 68-91, Jan. 1968.
2. Edwards, I. and Jansson, R.E.W., "Gasdynamics of Resistojets," Journal of the British Interplanetary Society, Vol. 24, 1971, pp. 729-742.
3. Zafran, S. and Jackson, B., "Electrothermal Thruster Diagnostics," TRW-39152-6012-UE-00-Vol-2, TRW Systems Inc., Redondo Beach, CA, May 1983. (NASA CR-168174-Vol-2).
4. McKeivitt, F.X., "Design and Development Approach for the Augmented Catalytic Thruster (ACT)," AIAA Paper 83-1255, June 1983.
5. Penko, P.F., Manzella, D.H., Dewitt, K.J., and Keith, D.G., "Effect of Ambient Pressure on the Performance of a Resistojet," AIAA Paper 87-0991, May 1987.

6. Spisz, E.W., Brinich, P.F., and Jack, J.R., "Thrust Coefficients of Low-Thrust Nozzles," NASA TN D-3056, 1965.
7. Nickerson, G.R., Coats, D.E., and Dang, L.D., "Engineering and Program Manual TDK," SN-63, Software and Engineering Associates Inc., Carson City, NV, Apr. 1985. (NASA CR-178628).
8. Sovey, J.S., Penko, P.F., Grisnik, S.P., and Whalen, M.V., "Vacuum Chamber Pressure Effects on Thrust Measurements of Low Reynolds Number Nozzles," Journal of Propulsion and Power, Vol. 2, No. 5, Sept. - Oct. 1986, pp. 385-389.
9. Teledyne Hastings-Raydist, Catalog 500H, Mini-Flow Calibrator, Specification Sheet No. 520B, Aug. 1984.
10. Back, L.H., Massier, P.F., and Gier, H.L., "Comparison of Measured and Predicted Flows Through Conical Supersonic Nozzles, with Emphasis on the Transonic Region," AIAA Journal, Vol. 3, No. 9, Sept. 1965, pp. 1606-1614.
11. Back, L.H., Cuffel, R.F., and Massier, P.F., "Influence of Contraction Section Shape and Inlet Flow Direction on Supersonic Nozzle Flow and Performance," Journal of Spacecraft and Rockets, Vol. 9, No. 6, June 1972, pp. 420-427.
12. Massier, P.F., Back, L.H., Noel, M.B., and Sahell, F., "Viscous Effects on the Flow Coefficient for a Supersonic Nozzle," AIAA Journal, Vol. 8, No. 3, March 1970, pp. 605-607.
13. Rothe, D.E., "Electron-Beam Studies of Viscous Flow in Supersonic Nozzles," AIAA Journal, Vol. 9, No. 5, May 1972, pp. 804-811.
14. Rae, W.J., "Some Numerical Results on Viscous Low-Density Nozzle Flows in the Slender-Channel Approximation," AIAA Journal, Vol. 9, No. 5, May 1972, pp. 811-820.

TABLE 1. - NOZZLE PARAMETERS

Nozzle	Shape	Exit half-angle		Throat diameter, mm	Area ratio
		Throat	Exit plane		
1	Conical	20°	20°	0.653	120:1
2	Bell	35°	20°	.711	150:1
3	Trumpet	0°	36°	.671	125:1
4	Modified trumpet	15°	28°	.640	135:1

TABLE 2. - NOZZLE CHARACTERISTICS AT A REYNOLDS NUMBER OF 1000 FOR NITROGEN AND HYDROGEN

Nozzle	Shape	Discharge coefficient, $C_D$		Specific impulse efficiency, $\eta_{ISP}$		Thrust coefficient, $C_F$	
		Nitrogen	Hydrogen	Nitrogen	Hydrogen	Nitrogen	Hydrogen
1	Conical	0.87	0.88	0.80	0.78	1.18	1.17
2	Bell	.91	.92	.85	.75	1.31	1.17
3	Trumpet	.88	.86	.83	.78	1.24	1.14
4	Modified trumpet	.93	.93	.84	.76	1.33	1.20
-	Orifice plate	.98	.94	.58	.59	.97	.94

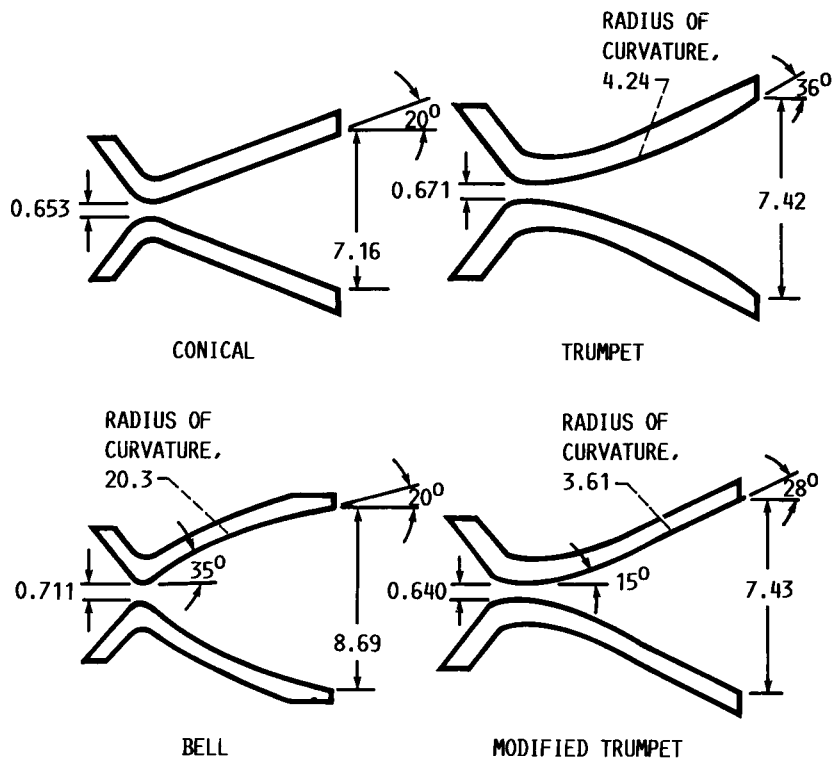
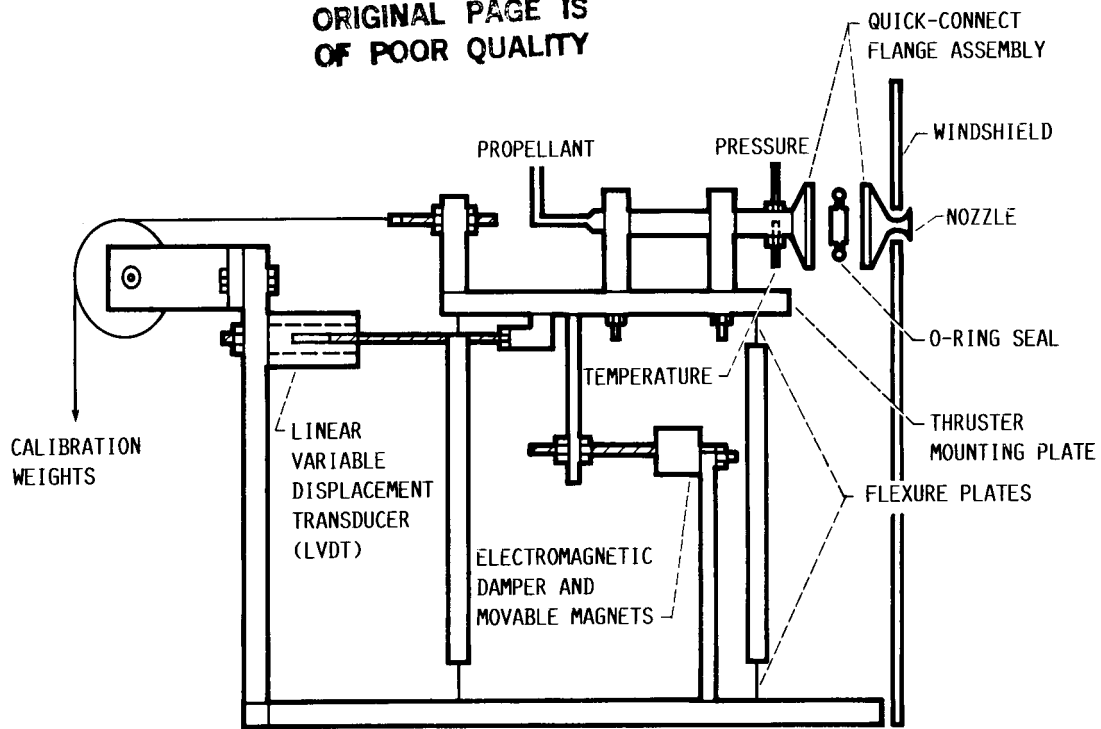
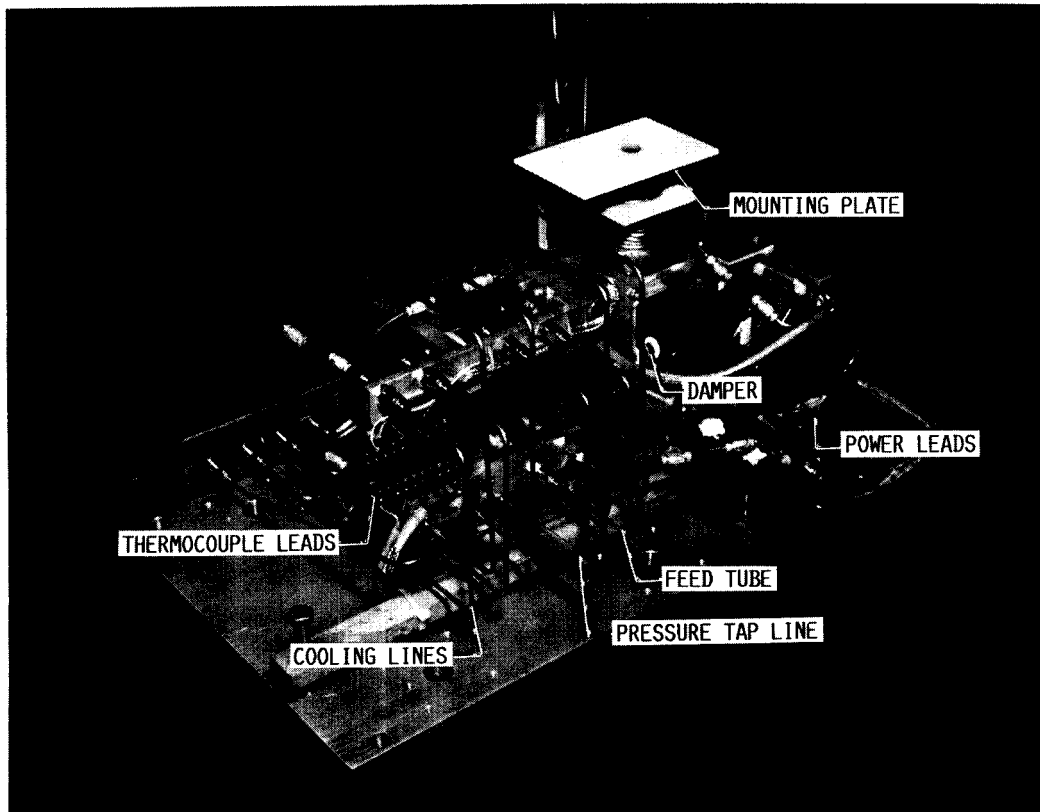


FIG. 1. - NOZZLE GEOMETRIES. ALL DIMENSIONS ARE IN MILLIMETERS.

ORIGINAL PAGE IS  
OF POOR QUALITY



(A) SCHEMATIC OF NOZZLE ASSEMBLY AND THRUST STAND.



(B) THRUST STAND.

FIG. 2. - NOZZLE ASSEMBLY AND THRUST STAND.

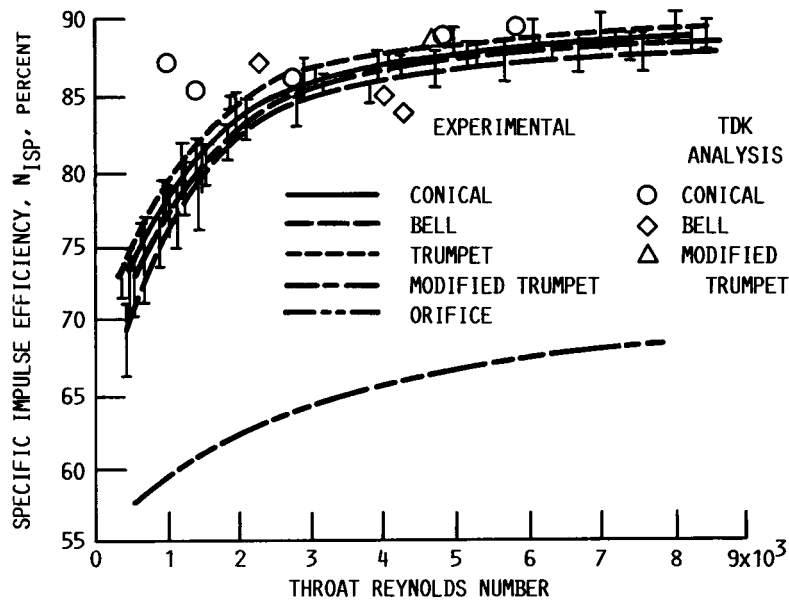


FIG. 3. - SPECIFIC IMPULSE EFFICIENCY AS FUNCTION OF THROAT REYNOLDS NUMBER FOR HYDROGEN. EXPERIMENTAL DATA AND TWO-DIMENSIONAL KINETICS (TDK) NOZZLE ANALYSIS.

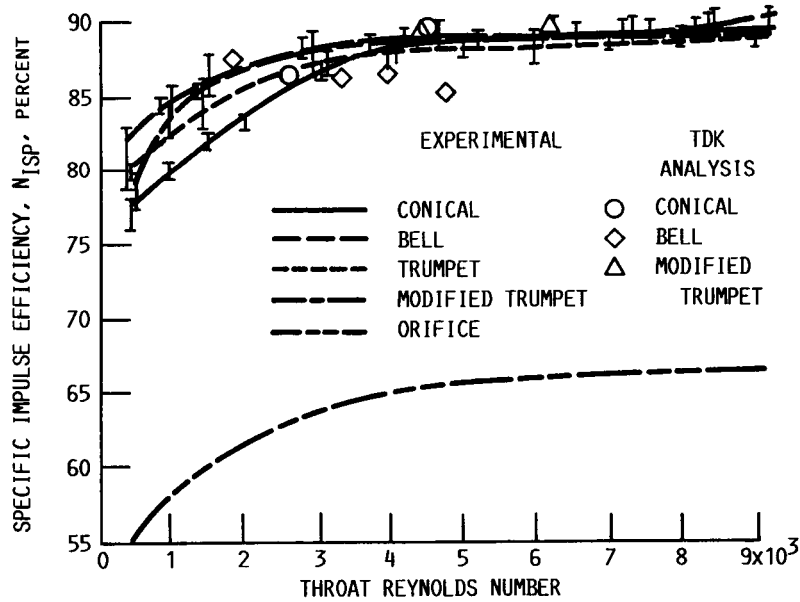


FIG. 4. - SPECIFIC IMPULSE EFFICIENCY AS FUNCTION OF THROAT REYNOLDS NUMBER FOR NITROGEN. EXPERIMENTAL DATA AND TWO-DIMENSIONAL KINETICS (TDK) NOZZLE ANALYSIS.

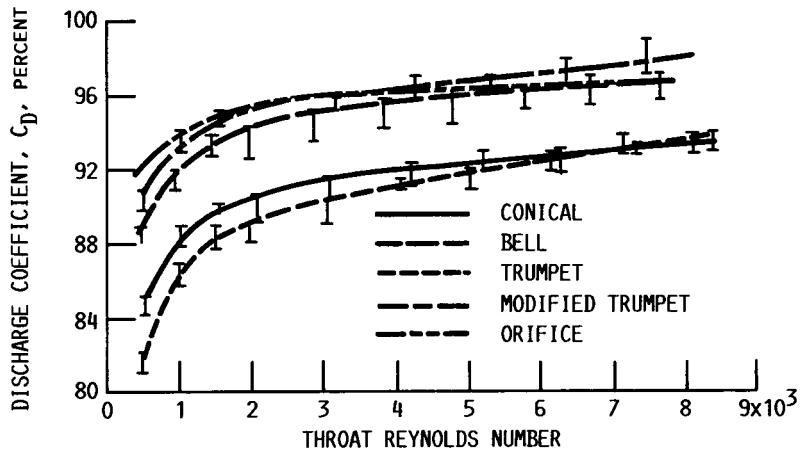


FIG. 5. - DISCHARGE COEFFICIENT AS FUNCTION OF THROAT REYNOLDS NUMBER FOR HYDROGEN.

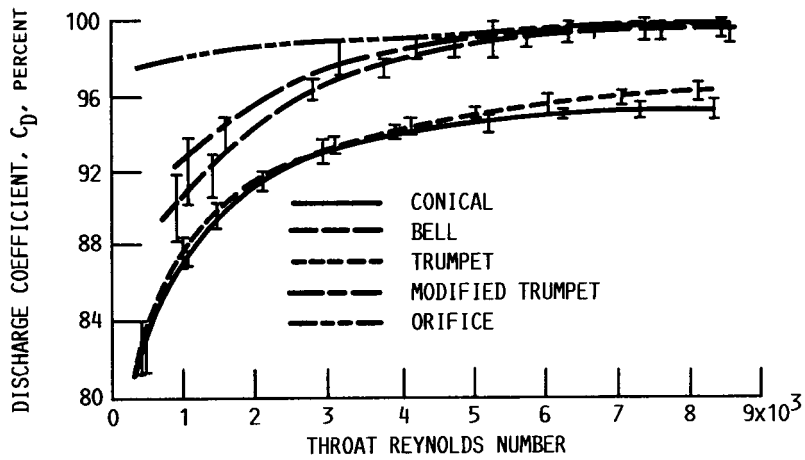


FIG. 6. - DISCHARGE COEFFICIENT AS FUNCTION OF THROAT REYNOLDS NUMBER FOR NITROGEN.

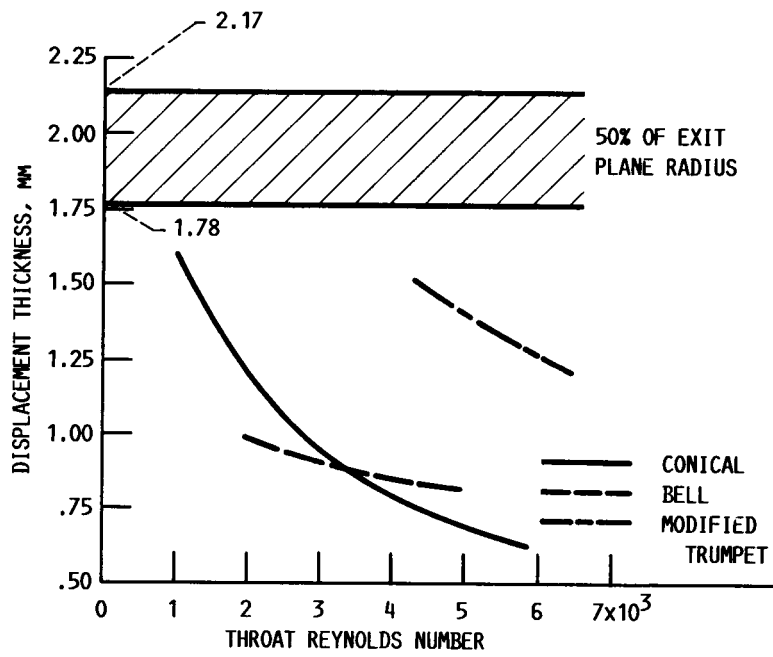


FIG. 7. - TWO-DIMENSIONAL KINETICS (TDK) NOZZLE ANALYSIS  
 PREDICTED DISPLACEMENT THICKNESS AS FUNCTION OF REYNOLDS  
 NUMBER AT EXIT PLANE FOR NITROGEN AND HYDROGEN.

1. Report No. <b>NASA TM-89858 AIAA-87-0992</b>		2. Government Accession No.		3. Recipient's Catalog No.	
4. Title and Subtitle  <b>Experimental Study of Low Reynolds Number Nozzles</b>				5. Report Date	
				6. Performing Organization Code  <b>506-42-31</b>	
7. Author(s)  <b>Stanley P. Grisnik, Tamara A. Smith, and Larry E. Saltz</b>				8. Performing Organization Report No.  <b>E-3526</b>	
				10. Work Unit No.	
9. Performing Organization Name and Address  <b>National Aeronautics and Space Administration Lewis Research Center Cleveland, Ohio 44135</b>				11. Contract or Grant No.	
				13. Type of Report and Period Covered  <b>Technical Memorandum</b>	
12. Sponsoring Agency Name and Address  <b>National Aeronautics and Space Administration Washington, D.C. 20546</b>				14. Sponsoring Agency Code	
15. Supplementary Notes <b>Prepared for the 19th International Electric Propulsion Conference cosponsored by the AIAA, DGLR, and JSASS, Colorado Springs, Colorado, May 11-13, 1987. Stanley P. Grisnik and Tamara A. Smith, NASA Lewis Research Center; Larry E. Saltz, Rocket Research Company, Redmond, Washington 98052-1012.</b>					
16. Abstract  <b>High-performance electrothermal thrusters operate in a low nozzle-throat Reynolds number regime. Under these conditions, the flow boundary layer occupies a large volume inside the nozzle, contributing to large viscous losses. Four nozzles (a conical, bell, trumpet, and modified trumpet) and a sharp-edged orifice were evaluated over a Reynolds number range of 500 to 9000 with unheated nitrogen and hydrogen. The nozzles showed significant decreases in specific impulse efficiency with decreasing Reynolds number. At Reynolds numbers less than 1000, all four nozzles were probably filled with a large boundary layer. The discharge coefficient decreased with Reynolds number in the same manner as the specific impulse efficiency. The bell and modified trumpet nozzles had discharge coefficients 4 to 8 percent higher than those of the cone or trumpet nozzles. The Two-Dimensional Kinetics (TDK) nozzle analysis computer program was used to predict nozzle performance. The results were then compared to the experimental results in order to determine the accuracy of the program within this flow regime.</b>					
17. Key Words (Suggested by Author(s)) <b>Low Reynolds numbers Nozzles Discharge coefficients Electrothermal propulsion</b>			18. Distribution Statement <b>Unclassified - unlimited STAR Category 20</b>		
19. Security Classif. (of this report) <b>Unclassified</b>		20. Security Classif. (of this page) <b>Unclassified</b>		21. No. of pages <b>12</b>	22. Price* <b>A02</b>